Topological Descriptors of the Electron Density and the Electron Localization Function in Hydrogen Bond Dimers at Short Intermonomer Distances

Luis F. Pacios[†]

Unidad de Química, Departamento de Biotecnología, E.T.S. Ingenieros de Montes, Universidad Politécnica de Madrid, E-28040 Madrid, Spain

Received: August 15, 2003; In Final Form: December 1, 2003

Geometries for five dimers linked by O−H···O hydrogen bonds (HBs) are optimized in MP2/6-311++G-(d,p) ab initio calculations for several short intermonomer distances *R*. Several molecular descriptors obtained from the topology of the electron density $\rho(\mathbf{r})$ and electron localization function $\eta(\mathbf{r})$ gradient fields are obtained at these geometries. Changes with *R* of topological descriptors of $\rho(\mathbf{r})$ and $\eta(\mathbf{r})$ show that they continue to exhibit features characteristics of strong hydrogen bonding even at distances shorter than equilibrium R_{eq}. Only at very short *R* where unstable dissociative structures appear do they exhibit features clearly indicative of weak interaction. Hence, topological indices of $\rho(\mathbf{r})$ and $\eta(\mathbf{r})$ fail to identify unambiguously R_{eq} among other distances within a given HB system.

Introduction

Hydrogen bonding has been the subject of an active field of research for nearly one century. This continued interest is easy to understand if one considers the crucial role played by hydrogen bonds (HBs) not only in condensed phases but also in many chemical and biological processes.[1−3] The coming to light of new types of HBs covering a wide range of interaction energies[4−16] and new data accumulated since around 1990 have changed the understanding of this interaction in the past decade. Among systems with weak energies, nonconventional HBs such as inverse hydrogen bonding, dihydrogen bonds, or H···π bonds[5] are responsible for new types of complexes posing challenging problems in solid state and protein chemistry[6,7] just to mention two major fields. As for systems with larger interaction energies, strong HBs[8−16] have received much attention in recent years especially due to their proposed role in several enzymatic mechanisms.[16−20] Strong bonds formed within active sites should provide enough energy to explain the large rate enhancements observed in many enzyme mechanisms, and besides, they should affect locally the pK_a's of amino acids enhancing the acidity of, otherwise weak, carbon acids.[14,15]

Hydrogen bonding systems A−H···B inherently involve the sharing of the H atom to varying extents between A and B which, in turn, can be related to the intermolecular distance. In conventional HBs, hydrogen is associated with either A or B so that the potential energy profile for the process A−H···B → A···H−B presents two wells separated by a noticeable barrier. When the A···B distance is short enough, the HB can display equal sharing of H between A and B (which may be depicted as A···H···B), the system presents a single well, and the H-transfer process is barrierless. However, for intermediate distances the energy profile for the change from A−H···B to A···H−B can show two wells separated by a low barrier. These low-barrier HBs (LBHBs) were observed in the gas phase long ago[21] whereas their possible existence in the interior of proteins in enzyme activity was first put forth in 1994,[19] its proposal being accepted since then by some authors[17,18,20,22] and rejected by others.[23,24]

When one tries to elucidate the physical nature of hydrogen bonding in such distinct complexes, a central issue is to identify what are the essential fingerprints of the interaction and how they change with the intermolecular distance. We have recently added to this research by studying the variation with the distance of properties relevant to the formation of dimers with one HB[25,26] and two HBs[27] (the reader can find an account of the most recent theoretical studies on the nature of hydrogen bonding in the introduction of refs 26 and 27 and references therein). From a epistemological point of view, it should be highly desirable to encompass physical quantum treatments of HB systems with chemical concepts such as bonds and electron lone pairs traditionally settled by chemists on the basis of empirical evidence. This goal can currently be accomplished thanks to conceptual frameworks developed around the electron density (ED), $\rho(\mathbf{r})$, and the electron localization function (ELF), $\eta(\mathbf{r})$.

The theory of atoms in molecules (AIM) of Bader[28,29] uses the gradient dynamical system of the ED to define basins of attractors achieving the partitioning of the molecular space into atomic domains. This theory has proven invaluable to characterize hydrogen bonding not only on theoretical EDs but also on experimentally determined EDs.[30,31] Furthermore, Popelier has proposed a set of AIM criteria that must be fulfilled by the hydrogen atom to characterize an intermolecular link as a true HB.[32] We have investigated the validity of these criteria under nonequilibrium situations as well as their fulfillment by A and B atoms involved in the HB.[26,27] The current status of the AIM theory is one of a firmly established methodology, and the conceptual picture displayed by the topological features of $\rho(\mathbf{r})$, local energy densities, and other related properties is largely independent of the particular approach used to obtain the ED itself.[30,31]

Bader's theory does not supply, however, explicit bond or lone electron pair basins although the Laplacian of $\rho(\mathbf{r})$ can be used for identifying these regions within the whole electron distribution of the system. That purpose can be accomplished with the gradient of the ELF, a function originally devised by Becke and Edgecomb to provide an orbital independent description of electron localization.[33] The topological analysis of the

[†] E-mail: lpacios@montes.upm.es.

10.1021/jp030978t CCC: $27.50
Published on Web 01/22/2004

ELF gradient field yields basins that partition the molecular space conveying the chemical picture of electron pairs, lone or bonded. The original work of Silvi and Savin[34] on the ELF gave place to a fruitful field of applications on a variety of molecular problems[34−39] including some HB systems[36−38] in last years.

In this paper, we apply these theoretical tools to explore the behavior of electron properties at short intermolecular distances in O−H···O bonds, which, together with O−H···N, are the most important strong HBs in proteins. One major characteristic of strong HBs is the short distance between heteroatoms, where *short* means usually <2.6 Å,[14] when both are oxygens, as has been observed in most enzyme/substrate complexes for which the LBHB hypothesis has been so far proposed.[20] Mildvan et al.[17] have used NMR proton chemical shifts, D/H fractionation factors, and solvent exchange rate data in enzymes for which high precision (±0.05Å) structures are available to detect short strong HBs and determine their heteroatom distances, finding lengths from 2.45 to 2.65 Å.[17] It is interesting to contrast this range with recent results by Kuo et al.[11] on large clusters of water molecules. In their study of processes occurring in the interface between ice and liquid water, these authors found that the HB topology has a large effect on the energy of clusters and observed spontaneous self-dissociation of one or more water molecules in some spatial arrangements. Grouping the types of HBs according to breaking of clusters, they reported a major class with the largest stability defined by the shortest O···O distances between 2.43 and 2.61 Å.[11]

In AIM studies intended to disclose the nature of hydrogen bonding a particularly useful idea is the partial covalent character that can be determined for a strong HB.[16,40] We have recently reported the change with intermolecular distance of a number of $\rho(\mathbf{r})$-dependent descriptors regarding the electrostatic/covalent character of HBs.[26,27] Relationships between topological features of the ED as well as values of local kinetic and potential energy density at the HB critical points and the associated distances in terms of strength of the HB have also been published in recent years.[41−44] However, one must bear in mind that no matter the electron features displayed, decreasing the heteroatom distance below its equilibrium value must only weaken the HB as far as the nature of the donor and acceptor is not changed. Theoretical analyses using the ED and ELF as sources of information are expected to cast light into the nature of strong HBs and LBHBs of increasing complexity in biomolecular systems soon. In this work, we apply these techniques to the study of neutral dimers linked by O−H···O bonds at short intermonomer distances. After a brief presentation of the methods employed, we discuss the results of these analyses on five model HB dimers. Structural changes and energies, ED properties and the information provided by basins of the ELF are considered separately and then our conclusions are gathered in the last section.

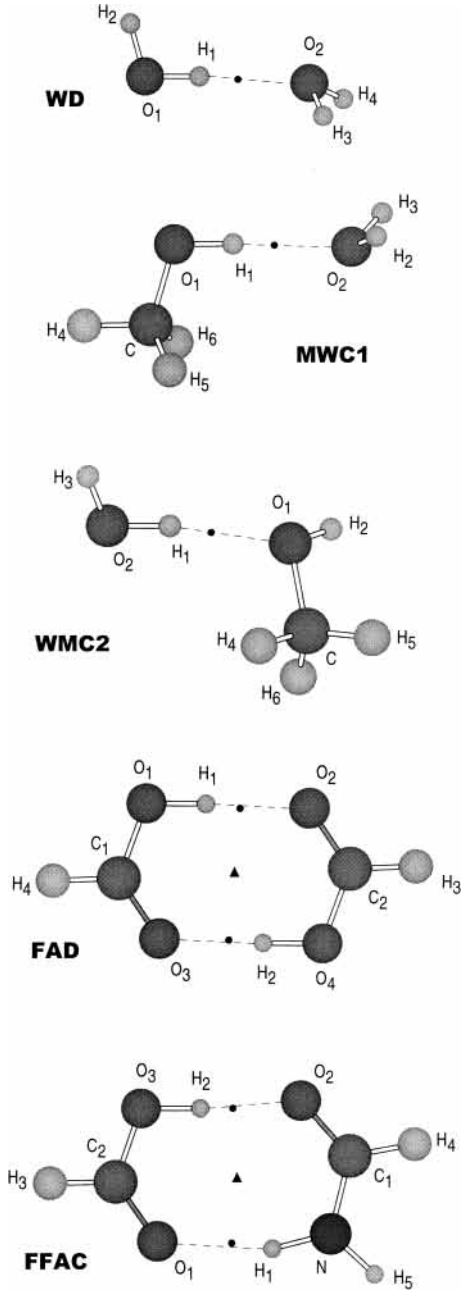

Figure 1. MP2/6-311++G(d,p) optimized equilibrium geometries for water dimer (WD), H-donor methanol/water complex 1 (MWC1), H-donor water/methanol complex 2 (WMC2), formic acid dimer (FAD), and formamide/formic acid complex (FFAC). Small circles indicate the location of bond critical points (BCPs) of $\rho(\mathbf{r})$ at the H-bonds (dashed lines). Small triangles in the cyclic plane dimers indicate the location of ring critical points (RCPs) of $\rho(\mathbf{r})$.

Methods

The following neutral dimers with O−H···O hydrogen bonds were studied: (i) water dimer (WD), (ii) H-donor methanol/water complex 1 (MWC1), (iii) H-donor water/methanol complex 2 (WMC2), (iv) formic acid dimer (FAD), and (v) formamide/formic acid complex (FFAC). Geometries were fully optimized without symmetry constraints in redundant internal coordinates at the MP2/6-311++G(d,p) level of theory keeping standard convergence criteria on displacements and forces for analytic gradients. Equilibrium geometries are displayed in Figure 1 where the atom numbering used throughout the paper is also indicated. Once the equilibrium geometries were found, a set of four additional structures were generated for every system as follows. In dimers with one single O−H···O bond (WD, MWC1, and WMC2) geometries were optimized by fixing the O···O intermolecular separation at 0.2 Å longer and 0.2, 0.4, and 0.6 Å shorter than the equilibrium value. In cyclic FAD (two O−H···O bonds) and FFAC (O−H···O and N−H···O bonds) these four additional geometries were obtained using instead the C···C distance, which makes the nonplanar structures found easier to analyze at the close intermonomer separations discussed below. Electron densities were then obtained in single point MP2/6-311++G(d,p) calculations at the five optimized structures of each system constraining tight convergence in the SCF cycle. All the geometries and EDs were obtained with GAUSSIAN98.[45]

Bond critical points (BCPs) of EDs as well as ring critical points (RCPs) appearing in cyclic systems such as FAD and FFAC were located and characterized with the program EXTREME[46] according to the prescriptions of AIM theory.[28,29] Figure 1 shows the position of BCPs at hydrogen bond paths (small circles) and RCPs (triangles) in equilibrium geometries. Local values of electron densities and electrostatic potentials at the H nucleus (see below) were calculated with CHECKDEN,[47] a program to compute and handle $\rho(\mathbf{r})$ and other related functions at different grids in molecular systems. Spatial grids of the ELF computed with the MP2/6-311++G(d,p) molecular orbitals, the topological analysis to obtain the basins of its gradient field and basin integrated properties (volume, electron population, and standard deviation) were calculated with the TOPMOD package.[48] A step interval of 0.07 bohr was chosen in each direction to set the spatial grids of ELF basins, which required between about 5.0×10^6 points for each one of WD structures and about 7.3×10^6 points for every FFAC geometry. Three-dimensional images of isosurfaces of ELFs were prepared with JMAP3D,[49] a freeware JAVA program that polygonizes volumetric data rendering VRML files (an in-house FORTRAN routine was written to convert TOPMOD output to JMAP3D input).

Results and Discussion

Geometries and Energies. Except for FFAC, for which our recent work[27] is the only theoretical treatment so far available, dimers depicted in Figure 1 have been common model systems in HB studies so that their equilibrium geometries and dissociation energies have been thoroughly discussed. The reader may find an updated review on ab initio and DFT results for accurate geometries, frequencies, and dissociation energies compared with recent experimental data in refs 26 and 27. Geometry changes with the intermonomer distance were discussed by us before,[26,27] but short distances such as those mentioned in the Introduction with regard to strong HBs were not fully analyzed. Ab initio geometry parameters of O−H···O hydrogen bonds for the five geometries of each system are collected in Table 1 along with dipole moments and relative energies. No energy correction was made for basis set superposition error (BSSE) because (a) we are here interested in differences between structures very far from dissociation and hence nearly equal BSSEs are expected at these distances and (b) we have already reported accurate dissociation energies for these complexes including the counterpoise correction to treat BSSE.[26,27] We begin focusing on the first three geometries of every dimer in Table 1 and then discuss the other ones.

The first row of each system in Table 1 corresponds to the only O···O distance longer than the equilibrium distance, the second row is the equilibrium one, and the third row is the immediate shorter distance. The lengthening of the A−H bond in the H-donor monomer is a well-known hydrogen bonding effect whose magnitude usually correlates well with the strength of the interaction.[1−4,40,41] Taking the O−H bond length from MP2/6-311++G(d,p) geometries for the isolated monomers (results not shown) and the intramolecular R(O−H) values of H-donors in Table 1, the O−H bond elongations are (Å) 0.0061 for WD, 0.0049 for MWC1, 0.0081 for WMC2, 0.0208 for FAD, and 0.0253 for FFAC. This sequence of values is in agreement with the HB strength reported for these dimers[26,27] (available experimental data or best theoretical estimates in kcal/mol): 5.0, 4.7, 5.4, 14.1, and 14.3, respectively. The magnitude of R(O−H) changes very little along the first three geometries in single-HB systems whereas cyclic dimers show slightly larger

TABLE 1: MP2/6-311++G(d,p) Geometry Parameters (Bond Lengths R in Å, Bond Angles θ in Degrees) of O−H···O Hydrogen Bonds, Dipole Moments (μ in Debye), and Relative Energies (ΔE in kcal/mol) for Five Intermolecular Distances of the HB Systems Displayed in Figure 1

R(O···O)	R(O−H)	R(H···O)	θ(HOO)	μ	ΔE
		WD			
3.1	0.9654	2.135	0.53	3.28	0.30
2.914[a]	0.9656	1.950	2.27	3.29	0
2.7	0.9647	1.743	5.65	3.25	0.78
2.5	0.9613	2.123	56.3	0.81	2.6
2.3	0.9598	1.977	58.6	0.05	6.3
		MWC1			
3.1	0.9645	2.136	1.36	3.20	0.32
2.906[a]	0.9643	1.942	1.26	3.34	0
2.7	0.9630	1.737	0.64	3.53	0.75
2.5	0.9595	1.546	4.87	3.48	4.0
2.3	0.9597	1.960	57.6	0.35	6.3
		WMC2			
3.0	0.9673	2.037	4.42	3.05	0.22
2.856[a]	0.9676	1.894	5.25	3.11	0
2.6	0.9668	1.697	16.8	2.75	1.2
2.4	0.9625	1.625	28.9	2.32	5.0
2.2	0.9553	1.781	52.2	1.24	13.
		FAD			
2.856 ($R_{CC} = 4.0$)[b]	0.9839	1.872	0.8	0.0	0.53
2.715 ($R_{CC} = 3.84$)[a]	0.9898	1.726	1.2	0.0	0
2.523 ($R_{CC} = 3.6$)[b]	1.005	1.520	2.0	0.0	2.3
2.573 ($R_{CC} = 3.4$)[b]	0.9885	1.640	15.2	1.12	5.9
2.699 ($R_{CC} = 3.2$)[b]	0.9751	1.947	32.4	1.36	9.2
		FFAC			
2.794 ($R_{CC} = 4.1$)[b]	0.9890	1.808	3.7	2.98	0.46
2.685 ($R_{CC} = 3.95$)[a]	0.9943	1.692	2.7	3.00	0
2.588 ($R_{CC} = 3.8$)[b]	1.002	1.587	1.9	3.07	0.67
2.558 ($R_{CC} = 3.6$)[b]	0.9986	1.579	8.9	3.41	3.1
2.603 ($R_{CC} = 3.4$)[b]	0.9865	1.686	17.3	3.44	6.1

[a] Equilibrium geometry. [b] C···C distance fixed at the geometry optimization: see the text.

changes related to the fact that they are more tightly bound (notice the shorter O···O and H···O distances). The intermolecular θ(HOO) bond angle increases noticeably in the first three geometries only when the H-donor is water (WD and WMC2) whereas MWC1 and FAD exhibit essentially linear HBs (θ(HOO) near zero) and the two HBs in the FFAC heterodimer are constrained by the different geometry of individual monomers to be slightly bent (see Figure 1). Dipole moments along these three structures remain virtually constant whereas, as expected, the energy rises more rapidly at the shorter O···O length than at the outer one, despite the respective intervals around equilibrium being nearly equal. In light of these geometries and with two exceptions, the five systems behave similarly in keeping their structures essentially unaltered with energy changes within 1 kcal/mol associated with O···O separations from 3.1 to 2.6 Å. The first exception is WMC2 that shows at 2.6 Å a large increase in the HB angle (16.8°), which in turn makes its dipole moment decrease about 10% (yet the energy rises only 1.2 kcal/mol). Because this O···O length is 0.1 Å shorter than the other single-HB dimers, this particular feature may be viewed as a prelude to the great changes taking place when monomers are brought closer, discussed in the next paragraph. The second exception is FAD at R(C···C) = 3.6 Å with 2.3 kcal/mol above equilibrium. This large energy may be understood if one considers that this distance represents the closest proximity between monomers while the structure remains planar (μ null), as noticed in the values of R(O···O) and R(H···O), actually the shortest ones among cyclic geometries in Table 1.

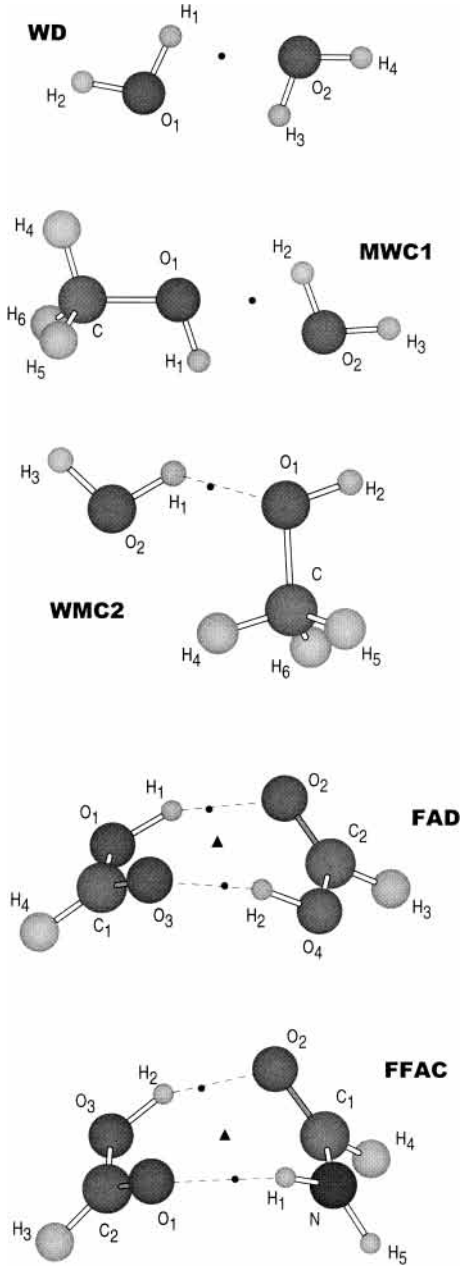

Figure 2. MP2/6-311++G(d,p) optimized nonequilibrium geometries for WD at $R(O_1\cdots O_2) = 2.5$ Å (equilibrium value $R_{eq} = 2.914$ Å), MWC1 at $R(O_1\cdots O_2) = 2.3$ Å ($R_{eq} = 2.906$ Å), WMC2 at $R(O_1\cdots O_2) = 2.4$ Å ($R_{eq} = 2.856$ Å), FAD at $R(C_1\cdots C_2) = 3.4$ Å ($R_{eq} = 3.843$ Å), and FFAC at $R(C_1\cdots C_2) = 3.4$ Å ($R_{eq} = 3.952$ Å). Small circles represent intermolecular BCPs and small triangles in cyclic dimers, RCPs. H···O hydrogen bonds are drawn as dashed lines only when the BCPs are near HB paths.

A dramatic change in geometries occurs then at the two shortest O···O distances in Table 1, as shown in the structures of Figure 2. WD presents at R(O···O) = 2.5 Å, an almost antiparallel arrangement (the value 2.123 Å refers to $H_1\cdots O_2$ whereas the $O_1\cdots H_3$ length is 2.042 Å and μ is small but not zero) with a noticeable decrease of the intramolecular O−H bond length with respect to previous values. At R(O···O) = 2.3 Å the O−H length is nearly that of isolated water (0.9595 Å), H_1 and H_3 atoms form equilateral triangles with both O_1 and O_2 ($O_1\cdots H_3$ distance is 1.966 Å, θ(HOO) ∼ 60°, and μ is essentially zero), and the structure is 6.3 kcal/mol above equilibrium. MWC1 shows at R(O···O) = 2.5 Å a geometry still similar to that of equilibrium except that the shortening of the O−H bond (this length is 0.9594 Å in isolated methanol) is a sign of the significant weakening of the interaction noticed in the value of ΔE. At R(O···O) = 2.3 Å this complex exhibits already a pattern completely similar to that of WD at the same distance: θ(HOO) ∼ 60° and ΔE = 6.3 kcal/mol. The small value of μ (0.35 D) indicates that this dipole moment is mostly due to the two hydroxyl bonds whereas methyl group in methanol acts much like the second hydrogen in water. The plane of water and the plane defined by CO_1H_1 atoms of methanol are out from coplanarity by about 5°. In WMC2 at R(O···O) = 2.4 Å the geometry still keeps the qualitative pattern of equilibrium (see θ(HOO) and μ) although the methyl group is closer to the O_2 molecule: compare the geometries of WMC2 in Figures 1 and 2. At a O···O distance of 2.2 Å, indeed the shortest one in Table 1, the great instability (ΔE = 13 kcal/mol) is noticed especially in the anomalous short O−H length, which reveals that geometry distortions, amplified at such a short separation, are felt mainly as a compression of the O−H bond. The angle between the plane of water and the plane defined by CO_1H_1 atoms is now 52.6°, which makes the dipole moment remain higher than in MWC1. On the basis of these results and taking into account that theoretical as well as experimental data point to dissociation energies about 5.0, 4.7, and 5.4 kcal/mol for WD, MWC1, and WMC2, respectively,[26] 2.3 Å should be considered an inner limit for the O···O distance in single-HB systems if gas phase destabilized structures exist above dissociaton. However, it should be stressed that even at such distances, an intermolecular BCP not very far from H···O paths is still found, as depicted in Figure 2 and analyzed below. It is interesting to contrast these results with some O−H···O systems in neutron diffraction crystal structures, for which extremely short O−H bonds with lengths in the range 0.77−0.86 Å at O···O distances between 2.71 and 2.83 Å have been observed.[44] Ab initio correlated calculations on model dimers for these systems show that they are energetically stable despite the anomalous short O−H bonds due to the HB interaction[44] (compare, however, their O···O distances with results in Table 1).

Cyclic dimers with two HBs become nonplanar when monomers are close enough, as we found before in B3LYP calculations.[27] Even the individual monomers lost then their plane geometry with both hydrogens in opposite sides out from COO plane in formic acid. However, the monomer HOCO dihedral angles are small: about 5° at the second shortest R_{CC} distance and 9° at the shortest one in both FAD and FFAC. As for intermolecular angles if we take for reference the OCO plane in formic acid monomers in FAD, the angle between planes is 119° at R_{CC} = 3.4 Å and 93° at 3.2 Å (this angle is 180° if both monomers were coplanar). If the OCN plane is now chosen in formamide, the equivalent angles in FFAC are 135° at R_{CC} = 3.6 Å and 89° at 3.4 Å. The dipole moment of the symmetrical homodimer FAD becomes nonzero as a consequence of this loss of planarity whereas in the heterodimer FFAC the equilibrium μ = 3 D value changes very little with the new spatial arrangement. Even at these strained geometries, the intramolecular O−H bond lengths remain noticeably larger than in isolated formic acid (0.9690 Å), and besides, ΔE values are still smaller than the dissociation energies reported for these dimers: between 12.5 and 14.8 kcal/mol depending on the level of theory or experimental technique for FAD and 14.3 kcal/mol (theoretical result) for FFAC.[27] Taken together, these results suggest that unlike single-HB dimers, the great geometry distortions upon close intermonomer approximations in two-HB cyclic dimers keep the stability due to the HB interaction. The fact that intermolecular BCPs (see below) are even then

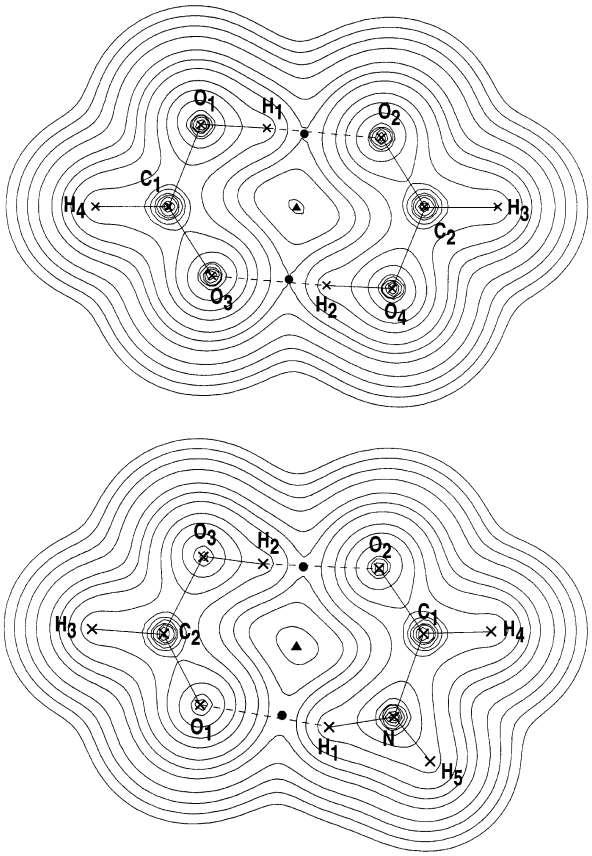

Figure 3. MP2/6-311++G(d,p) electron density contours maps for FAD (above) and FFAC (below) at the planes containing all the atoms in their equilibrium structures. Nuclear positions are indicated by crosses, intermolecular BCPs by circles and RCPs by triangles. The outermost contour is $\rho(\mathbf{r}) = 0.001$ au and the remaining contours equal 2×10^n, 4×10^n, and 8×10^n au, with $n = -3, -2, -1, 0, 1$, and 2. Atom numbering refers to Figure 1.

TABLE 2: Properties of the Bond Critical Point[a] of the MP2/6-311++G(d,p) Electron Density (ED) at the HB Path and Properties of the Hydrogen Nucleus in the HB (Electron Density ρ^0_H and Electrostatic Potential U^0_H) for Five O···O Intermolecular Distances of the HB Systems Displayed in Figure 1 (All Values in au Expect R(O···O) in Å)

R(O···O)	x_C	ρ_C	$\nabla^2\rho_C$	G_C	V_C	H_C	ρ^0_H	U^0_H
				WD				
3.1	0.358	0.0154	0.0579	0.0124	−0.0104	+0.0020	0.4017	−0.8583
2.914[b]	0.350	0.0231	0.0913	0.0205	−0.0182	+0.0023	0.3992	−0.8426
2.7	0.336	0.0379	0.1452	0.0367	−0.0371	−0.0004	0.3964	−0.8257
2.5		0.0214	0.1149	0.0241	−0.0195	+0.0046	0.4061	−0.9161
2.3		0.0287	0.1951	0.0401	−0.0315	+0.0086	0.4056	−0.9060
				MWC1				
3.1	0.360	0.0156	0.0578	0.0125	−0.0106	+0.0019	0.4062	−0.8499
2.906[b]	0.351	0.0238	0.0934	0.0212	−0.0190	+0.0022	0.4038	−0.8207
2.7	0.337	0.0385	0.1472	0.0375	−0.0382	−0.0007	0.4014	−0.7741
2.5	0.317	0.0627	0.2135	0.0651	−0.0768	−0.0117	0.4002	−0.7129
2.3		0.0299	0.1893	0.0398	−0.0322	+0.0076	0.4095	−0.9149
				WMC2				
3.0	0.352	0.0197	0.0736	0.0164	−0.0143	+0.0021	0.3984	−0.8721
2.856[b]	0.345	0.0270	0.1033	0.0241	−0.0224	+0.0017	0.3960	−0.8612
2.6	0.334	0.0430	0.1622	0.0427	−0.0449	−0.0022	0.3931	−0.8770
2.4	0.336	0.0521	0.2061	0.0563	−0.0610	−0.0047	0.3946	−0.8957
2.2	0.392	0.0424	0.2404	0.0545	−0.0489	+0.0056	0.4068	−0.9105
				FAD				
4.0[c]	0.342	0.0278	0.0977	0.0233	−0.0222	+0.0011	0.3723	−0.8070
3.84[b,c]	0.330	0.0401	0.1289	0.0348	−0.0375	−0.0027	0.3639	−0.7671
3.6[c]	0.305	0.0692	0.1726	0.0617	−0.0802	−0.0185	0.3479	−0.6945
3.4[c]	0.330	0.0494	0.1562	0.0455	−0.0519	−0.0064	0.3656	−0.7923
3.2[c]	0.378	0.0241	0.0965	0.0221	−0.0201	+0.0020	0.3853	−0.8682
				FFAC				
4.1[c]	0.335	0.0327	0.1095	0.0275	−0.0277	−0.0002	0.3654	−0.7889
3.95[b,c]	0.325	0.0438	0.1342	0.0379	−0.0422	−0.0043	0.3585	−0.7534
3.8[c]	0.313	0.0580	0.1564	0.0508	−0.0625	−0.0117	0.3508	−0.7146
3.6[c]	0.317	0.0583	0.1621	0.0522	−0.0639	−0.0117	0.3548	−0.7530
3.4[c]	0.338	0.0432	0.1460	0.0400	−0.0435	−0.0035	0.3685	−0.8040

[a] Location of the BCP given as fraction of the H···O distance x_C, value of ED ρ_C, Laplacian of ED $\nabla^2\rho_C$, kinetic energy density G_C, potential energy density V_C, and total energy density H_C. [b] Equilibrium geometry. [c] C···C distance.

located quite close to H···O paths (see Figure 2) lends further support to this observation.

Electron Densities. The existence of a (3,−1) BCP of the electron density at H···B paths ($\rho(\mathbf{r})$ minimum along the line joining H and B atoms, maximum at the other two orthogonal directions) is one essential feature of A−H···B hydrogen bonding. The topological properties of this BCP are the subject of AIM criteria proposed to characterize the interaction.[28−32] Figure 3 displays contour maps of $\rho(\mathbf{r})$ showing the location of these BCPs in FAD and FFAC: see how the contour 0.04 au is broken at the BCPs, illustrating the minimum value of $\rho(\mathbf{r})$ there. When several bond paths form a closed ring, there appears a (3,+1) ring critical point, RCP, ($\rho(\mathbf{r})$ maximum along one direction and minimum at the other two orthogonal directions), also shown in Figure 3. Much theoretical effort has been devoted in recent years to relate these topological descriptors with the strength of HBs: the reader is referred to the exhaustive bibliographic compilations by Popelier et al.[30,31] The local value of $\rho(\mathbf{r})$ at the BCP, ρ_C, has been often treated as a measure of the HB strength because it correlates with HB energies.[4,41,50]

Table 2 gathers AIM properties of BCPs at H···O bond paths for the intermolecular distances considered in this work. In all cases, the BCP lies near the H atom at about one-third of the H···O line, approaching hydrogen more closely as the monomer separation is reduced before reaching the innermost distances. For the two shortest O···O lengths in WD and the shortest one in MWC1, the BCP is so far from the H···O line that it cannot be considered as a hydrogen bond critical point so that its location is not included in Table 2. However, an intermolecular BCP exists (see Figure 2) and its topological properties, though somewhat apart from general trends, show features similar to the rest of data. As noted by Popelier et al. in prescribing AIM criteria for HBs,[29,32] the order of magnitude of ρ_C is about 10^{-2} au, being larger as H···O lengths become shorter. Thus, equilibrium values for the five systems studied here obey the equation $\rho_C = 0.177 - 0.0788R$(H···O), $r = 0.9990$ (the correlation with R(O···O) is a bit worse, with $r = 0.9978$) in good agreement with the correlation reported by Alkorta and Elguero, $\rho_C = 0.19-0.08R$(H···N), $r = 0.994$, for 38 A−H···N bonds (A = C, N, O, F) existing in α-amino alcohols selected to study self-discrimination of enantioners in HB dimers.[42] However, it must be stressed that ρ_C still increases at distances shorter than that at equilibrium (see, for instance, MWC1 at 2.5 Å, WMC2 at 2.4 Å, or FAD and FFAC at 3.6 Å), where energy rises rapidly, and that good linear correlations are still found at such inner distances. For instance, a correlation coefficient of 0.9991 is found for the set of values corresponding to the second shortest intermolecular lengths excluding WD. Hence, relationships between ρ_C and HB strengths should be used with caution. One must bear in mind that a larger value of $\rho(\mathbf{r}=\mathbf{x})$ should be always expected if, along a given bond line, $\mathbf{x}$ is closer to a nucleus, as is indeed the case with the position of BCPs with respect to H atom. If one considers the HB dissociation energies of these systems presented above, the relation between ρ_C and the HB strength may be used as a guide only when *distinct* dimers at their equilibrium geometries are

compared. A similar conclusion follows from previous results on neutron diffraction crystal structures with very short O−H bonds mentioned before, where ρ_C is found to increase at shorter H···O distances without linear correlation with HB energy.[44]

As we[26,27] and others[51] have recently reported, the Laplacian of $\rho(\mathbf{r})$ at the BCP $\nabla^2\rho_C$ increases after equilibrium when monomers move closer, reaches a maximum, and then falls off rapidly with the intermolecular separation becoming negative only at short distances typical of covalent bonding (see Figure 5 in ref 26). This increase with smaller H···O distances has been also observed in a recent comparative study of experimental and theoretical EDs for crystals of six complexes of amino acids with water.[52] Laplacian values in Table 2 are positive everywhere, indicating thus local depletion of charge, a known feature of noncovalent interactions such as hydrogen bonding.[28,29] Although $\nabla^2\rho(\mathbf{r})$ is an excellent probe to study electron distributions and its topology can be mapped onto electron pairs shells,[53] providing thus a physical basis for the VSEPR model,[54] *local* values such as $\nabla^2\rho_C$ convey no useful information to distinguish among different intermolecular distances within a given HB dimer.

Much more interesting is the information provided by local energy densities listed in Table 2. The sum of kinetic $G(\mathbf{r})$ (always positive) and potential $V(\mathbf{r})$ (always negative) energy densities defines the total energy density $H(\mathbf{r})$.[28] The sign of H at any point $\mathbf{x}$ depends thus on which contribution dominates locally there. If H_C denotes $H(\mathbf{r}=\mathbf{x})$ when $\mathbf{x}$ is a BCP, positive values of $H_C = G_C + V_C$ are typical of ionic and hydrogen bonds[26−29,40−42] whereas $H_C < 0$ characterizes covalent bonds.[28,29] Values of H_C less than zero reflect a dominance of V_C that may be viewed as the consequence of accumulated stabilizing electronic charge at the BCP, a property of covalent interactions. Nevertheless, negative H_C have been found in short HBs, which has led us to speak of *partially covalent* hydrogen bonds[16,40] in such cases. Thus, crystal structures of carboxylic acids and their salts,[16] enzymes complexed with reaction intermediate analogues,[16] gas-phase dimers at short intermolecular distances,[26,27] several phases of ice,[40] and many other complexes in the solid phase[41] as well as ylides containing N, O, and C atoms as H-acceptors with intermediate and strong HB energies[43] happen to show $H_C < 0$ in HB paths. Negative H_C are seen in Table 2 for the five systems although in WD there is one single case at 2.7 Å too small to be significant. For both methanol/water dimers, H_C at equilibrium shows conventional (positive) values but at the two inner distances negative values appear, especially large in MWC1 at 2.5 Å. In this case the close proximity of the BCP to the H atom (x_C is the smallest value in single-HB dimers) when the H-donor methanol is *pushed* at such a short distance should explain the great local dominance of potential energy effects in concordance with the large value of ρ_C. As for the cyclic dimers, both exhibit already at equilibrium $H_C < 0$, continue increasing their negative values at inner distances, and only at the shortest C···C lengths where geometry distortions begin to appear, decrease or become positive. These results call again for caution when relating negative H_C values with strength or stability of hydrogen bonding. As illustrated in Figure 4, there is a clear relationship between H_C and the proximity between BCPs and H atoms so that the balance between G_C and V_C depends to a great extent on the location of the critical point regardless the relative stability. Even nonplanar distorted structures of FAD at R(C···C) = 3.4 Å (open down triangle in Figure 4) and FFAC at 3.6 and 3.4 Å (open up triangles), have BCPs with $H_C < 0$ as a consequence of the short O···O lengths

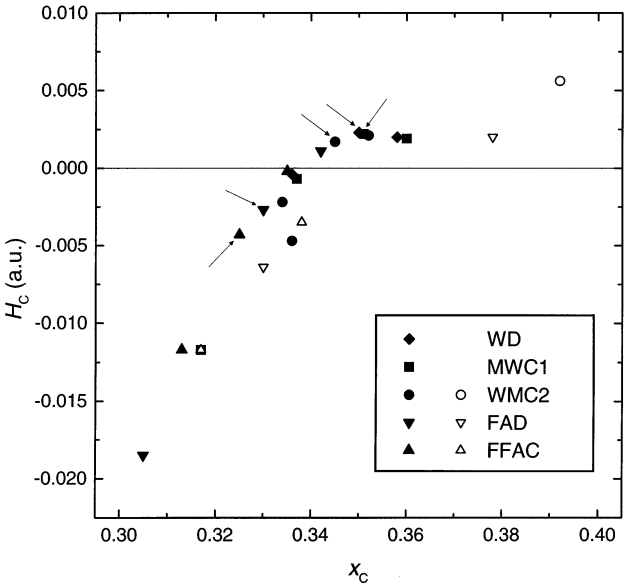

Figure 4. Total energy densities at BCPs in hydrogen bond paths, H_C, for the systems in Figure 1. The location of the BCP is given as fraction of the H···O distance, x_C. Open symbols for WMC2, FAD, and FFAC correspond to their distorted structures at short intermolecular distances (see Figure 2). The equilibrium geometry of every dimer is indicated by an arrow.

(see Table 1), keeping thus features of partially covalent HBs despite being far from equilibrium.

The red shift in frequencies of A−H vibrations associated with the lengthening of this bond upon formation of A−H···B links has been traditionally considered as evidence of HB formation.[1−3] In some HB systems, however, experiments have revealed that the A−H stretching vibration is shifted toward higher frequency, which has led us to speak of "blue-shifted" or "improper" hydrogen bonding in such cases; several detailed reports on blue-shifed HBs are available.[55−57] Although this effect was first observed for C−H bonds, recent studies suggest that blue-shifted HBs could be more general and may be observed in Si−H, P−H, and N−H bonds[56] and, under special circumstances, even in O−H bonds.[57] Nevertheless, on the basis of the recent theoretical model devised by Weinhold et al.[57] to explain improper HBs it seems unlikely that O−H···O systems such as those studied here could show blue shift. The elongation of O−H bonds observed above when geometries are discussed should then imply that the H atom of the H-donor suffers an electron deficiency[1,2] revealed when the ED at the H nucleus, ρ^0_H, in the complex is compared with the equivalent value in the monomer. This property is also listed along with the electrostatic potential at the H nucleus, U^0_H, in Table 2. The fundamental role of electrostatic potentials $U(\mathbf{r})$ to determine a variety of properties has been repeatedly demonstrated (for an updated discussion see the review by Politzer and Murray[58]) and exact relationships between $U(\mathbf{r})$ at nuclei, U^0, and total atomic and molecular energies have been known for thirty years.[59] Much more recently, values of $U(\mathbf{r})$ at selected atomic sites have been used as reactivity descriptors for hydrogen bonding.[60] Because the electrostatic potential at a nucleus is[58] $U^0 = -\int[\rho(\mathbf{r})/r]\, d\mathbf{r}$, the electron deficiency involved in hydrogen bonding must give rise to increased (less negative) values of U^0_H so that one should expect greater changes with respect to monomers in stronger HBs. Reference values (in au) for monomers computed at the same level of theory are the following. ρ^0_H: water, 0.4147; methanol, 0.4187; formic acid, 0.4006. U^0_H: water, −0.9515; methanol, −0.9695; formic acid,

−0.9241 (recall that exact atomic values for isolated hydrogen are $\rho^0 = \pi^{-1} = 0.3183$ and $U^0_H = -1$). Relative changes of ρ^0_H and U^0_H in single-HB dimers at equilibrium are very similar: decreases between 3.6 and 4.5% for the former property and increases between 9.5 and 15% for the latter. These relative differences are more noticeable in cyclic systems, about 10% for ρ^0_H and 18% for U^0_H, which indicates larger shifts of ED from hydrogen in these tighter bound dimers. With few exceptions, the trends observed in AIM descriptors are again followed by these two properties. Note how ED continues shifting from H, as shown by the smaller ρ^0_H and larger U^0_H values at the distances immediately shorter than that at equilibrium. At the closest separations where geometry distortions occur, the trends are again inverted and both ρ^0_H and U^0_H depart noticeably from previous values, becoming similar to those of isolated monomers, which hence indicates a loss of any stability in the interaction. As a final remark, it is worth emphasizing that all these $\rho(\mathbf{r})$-dependent descriptors happen to show features reminiscent of stronger HBs at intermolecular distances *shorter* than that at equilibrium, though upon even closer proximity where the systems become dissociative they change rapidly, separating from values characteristic of stable HB interactions.

Electron Localization Functions. Fuster and Silvi[38] have analyzed the topology of the ELF in several HB complexes and have established criteria to distinguish between weak, medium, and strong HBs. These criteria rely on local values of the ELF at BCPs as well as on electron population and its variance for the basins of the function deduced from the analysis of its gradient field[34] in a manner similar to that accomplished by AIM theory with the ED. We focus now on the variation with the intermonomer distance of descriptors supplied by the topology of the ELF to investigate whether this function provides more useful information to distinguish between different hydrogen bonding environments associated with distances shorter than that at equilibrium in the HB systems studied.

The ELF proposed by Becke and Edgecombe[33] can be written as

$$\eta(\mathbf{r}) = (1 + [(T - T_W)/T_{TF}]^2)^{-1} \qquad (1)$$

where T is the kinetic energy computed with the molecular orbitals, and T_W and T_{TF} are the von Weizsäcker (W) and Thomas−Fermi (TF) kinetic energy functionals, respectively.[61] Whereas the TF functional gives the kinetic energy of an electron gas with homogeneous density, the W functional obtained as (except a numerical factor) $[\nabla\rho(\mathbf{r})]^2/\rho(\mathbf{r})$ accounts for inhomogeneity corrections.[61] From a physical point of view, expression 1 has been interpreted in terms of local excess kinetic energy density, $T - T_W$, due to Pauli repulsion, giving thus a measure of the local electron localization in a system.[62] Because of the Lorentzian-type definition (1), the domain of the ELF is $0 \le \eta(\mathbf{r}) \le 1$. At spatial regions where there is either a single electron or an opposite spin electron pair, the Pauli repulsion has little influence and the excess local kinetic energy has a low value ($T \approx T_W$) so that $\eta(\mathbf{r})$ is close to 1. Contrarily, at the boundaries between such regions the probability of finding electrons with parallel spins is high, the excess local kinetic energy has a large value, and $\eta(\mathbf{r})$ approaches zero. The value $\eta(\mathbf{r}) = 1/2$ means $T = T_W \pm T_{TF}$, which represents a homogeneous electron gaslike pair probability, that is, electron delocalization. Volumes bounded by this $\eta(\mathbf{r})$ isosurface are displayed in Figures 5 and 6 for the systems studied at their equilibrium geometries. These domains trace separately just the bulk volume of monomers, but the distinct environment around the atoms involved in hydrogen bonding are highlighted. For instance, both oxygens in O−H···O show remarkable differences: see how the O atom in the H-donor is more compact than the acceptor O that exhibits in all cases two small protuberances associated with the lone electron pairs (see below), one of them pointing toward H in the H···O line. Hydrogens show even greater differences. Thus, whereas that involved in the HB has a tight domain that is always just a mere extension of the hydroxyl oxygen, the other hydrogens display large bulges, especially when bonded to carbon, a feature observed before in ELF studies.[35]

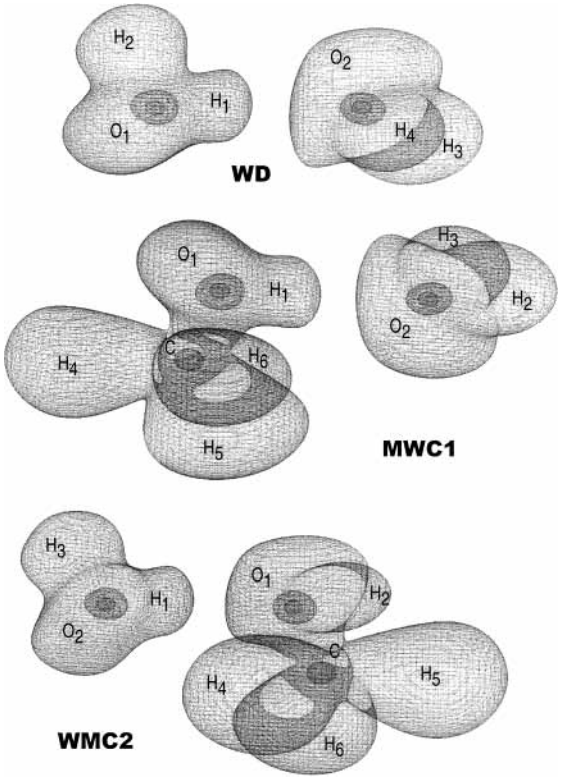

Figure 5. Spatial regions defined by the $\eta(\mathbf{r}) = 0.50$ isosurface for single-HB systems WD, MWC1, and WMC2 at equilibrium. Relative orientation and atom numbering as in Figure 1.

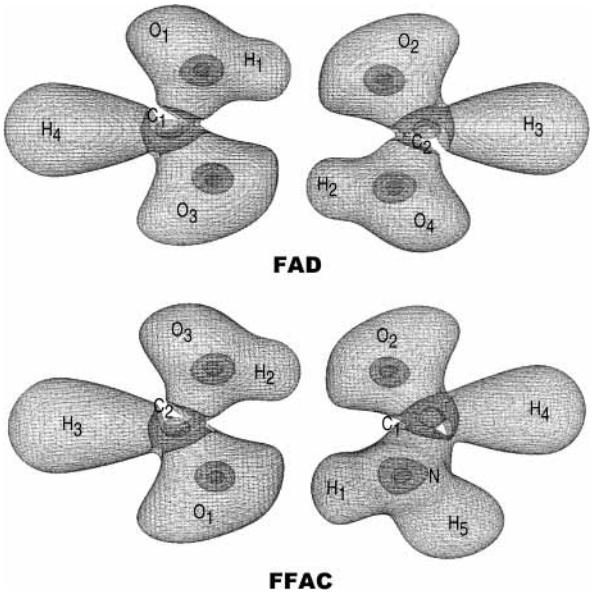

Figure 6. Spatial regions defined by the $\eta(\mathbf{r}) = 0.50$ isosurface for two-HB systems FAD and FFAC at equilibrium. Relative orientation and atom numbering as in Figure 1.

TABLE 3: Basins of the ELF Gradient Field Found at All the O···O Intermolecular Distances for the HB Systems Displayed in Figure 1[a]

core	disynaptic valence[b] (bond pairs)	monosynaptic valence (lone pairs)
	WD	
$C(O_1)$, $C(O_2)$	$\underline{V(H_1,O_1)}$, $V(H_2,O_1)$, $V(H_3,O_2)$, $V(H_4,O_2)$	$V(O_1)$, $V(O_1)$, $V(O_2)$, $V(O_2)$
	MWC1	
$C(O_1)$, $C(O_2)$, C(C)	$\underline{V(H_1,O_1)}$, $V(O_1,C)$, $V(H_2,O_2)$, $V(H_3,O_2)$, $V(H_4,C)$, $V(H_5,C)$, $V(H_6,C)$	$V(O_1)$, $V(O_1)$, $V(O_2)$, $V(O_2)$
	WMC2	
$C(O_1)$, $C(O_2)$, C(C)	$\underline{V(H_2,O_1)}$, $V(O_1,C)$, $V(H_1,O_2)$, $V(H_3,O_2)$, $V(H_4,C)$, $V(H_5,C)$, $V(H_6,C)$	$V(O_1)$, $V(O_1)$, $V(O_2)$, $V(O_2)$
	FAD	
$C(C_1)$, $C(C_2)$, $C(O_1)$, $C(O_2)$, $C(O_3)$, $C(O_4)$	$V(H_4,C_1)$, $V(O_1,C_1)$, $V(O_3,C_1)$, $V(H_3,C_2)$, $V(O_2,C_2)$, $V(O_4,C_2)$, $\underline{V(H_1,O_1)}$, $\underline{V(H_2,O_4)}$	$V(O_1)$,[c] $V(O_4)$,[c] $V(O_2)$, $V(O_2)$, $V(O_3)$, $V(O_3)$
	FFAC	
$C(C_1)$, $C(C_2)$, C(N), $C(O_1)$, $C(O_2)$, $C(O_3)$	$V(H_4,C_1)$, $V(O_2,C_1)$, $V(N,C_1)$, $V(H_3,C_2)$, $V(O_3,C_2)$, $V(O_1,C_2)$, $\underline{V(H_2,O_3)}$, $\underline{V(H_1,N)}$, $V(H_5,N)$	$V(N)$, $V(O_3)$,[c] $V(O_2)$, $V(O_2)$, $V(O_1)$, $V(O_1)$

[a] Atom numbering refers to this figure. [b] Disynaptic valence basins directly involved in hydrogen bonding are underlined. [c] Single monosynaptic basin containing two lone pairs.

Likewise in AIM theory, the topological analysis of the ELF gradient field yields critical points that enable partitioning of the molecular space into basins of attractors.[34] The ELF values at the critical points, η_C, define thus the electron localization domains of the system. The classification and features of those basins as well as their utility to determine a variety of molecular properties have been discussed in depth elsewhere[36−39] so we recall a very brief account of what is relevant here. In all cases, the critical points of $\eta(\mathbf{r})$ lie very close to the BCPs of $\rho(\mathbf{r})$ but whereas the partitioning of the space given by the topology of the ED yields atom basins, the topology of the ELF renders electron localization basins. There are mainly two types of basins named with conventional atomic electron structure terms: *core* basins around nuclei with $Z > 2$ and *valence* basins in the remaining space. Though a core basin is necessarily organized around one single atom, a valence basin is characterized by its synaptic order, defined as the number of cores to which it is connected. Core basins are labeled C(A) where A stands for the atomic symbol of the atom to which it belongs, whereas V(A,B) denotes a valence basin shared by A and B atoms and V(A) represents a valence basin containing one lone pair of atom A. For example, in water there is one core basin C(O), two disynaptic valence basins $V(O,H_1)$ and $V(O,H_2)$ and two monosynaptic valence basins corresponding to the two lone pairs of oxygen $V_1(O)$ and $V_2(O)$. The whole set of basins found at all the intermolecular distances considered for the HB systems studied are gathered in Table 3. Disynaptic valence basins belong to the intramolecular bond electron pairs whereas monosynaptic basins represent domains for the lone pairs of oxygens (one for nitrogen in FFAC) whose features are discussed below. It is worth remarking that oxygen in the H-donor formic acid monomer happens to show one single basin containing two lone pairs, as its population demonstrates (see below).

The partition of the molecular space in terms of domains of the ELF is frequently represented in graphical form by plotting volumes delimited by isosurfaces of $\eta(\mathbf{r})$ near 1 within which the Pauli repulsion is weak.[38] Because every basin is defined by the value of the ELF at its critical point $\mathbf{r}_C$, $\eta_C = \eta(\mathbf{r}=\mathbf{r}_C)$, these plots have to resort necessarily to one isocontour η_C value representative of the domains displayed. Our interest is focused on the features of the HB, and accordingly, we have chosen to render plots at a η value allowing for comparison of domains between dimers. For single-HB dimers WD, MWC1, and WMC2 the isocontour $\eta = 0.90$ chosen for Figure 7 represents within an interval of ± 0.01 units all the lone pair basins of oxygen atoms. The same criterion for two-HB dimers FAD and FFAC yields $\eta = 0.86$, which is the isocontour selected to render

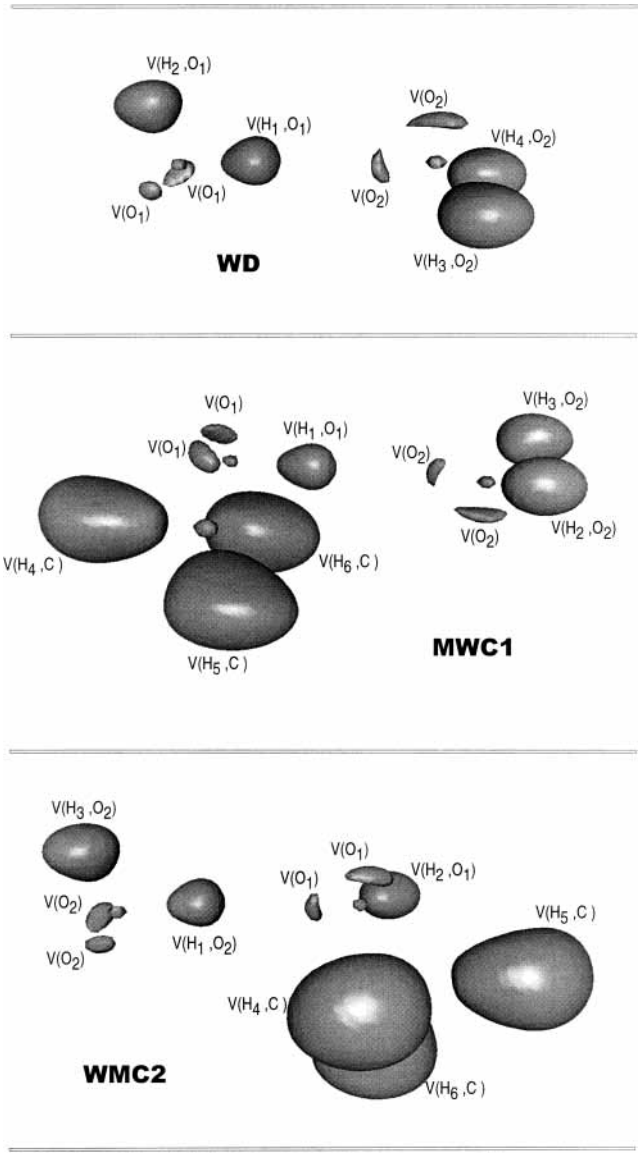

Figure 7. Localization domains ($\eta = 0.90$) of WD, MWC1, and WMC2 at equilibrium. Small unlabeled volumes at the location on oxygen and carbon atoms belong to core basins. Relative orientation and atom numbering as in Figure 1.

TABLE 4: ELF Valence Basin Properties at the HB[a]

	V(H,O)			V(O-donor)			V_1(O-acceptor at HB)			V_2(O-acceptor)		
R[b]	Vol	N_i	$\sigma(N_i)$	Vol	N_i	$\sigma(N_i)$	Vol	N_i	$\sigma(N_i)$	Vol	N_i	$\sigma(N_i)$
						WD						
3.1	33.6	1.76	0.17	66.5	2.22	0.24	42.2	2.15	0.10	64.5	2.27	0.28
2.91[c]	30.3	1.75	0.14	67.1	2.21	0.25	38.2	2.14	0.20	64.3	2.28	0.26
2.7	26.6	1.77	0.00	67.7	2.20	0.22	32.7	2.13	0.26	64.0	2.30	0.28
2.5	42.7	1.74	0.22	57.3	2.20	0.19	49.9	2.19	0.10	61.4	2.24	0.22
2.3	41.7	1.74	0.20	54.5	2.21	0.14	50.3	2.21	0.14	57.9	2.21	0.17
						MWC1						
3.1	31.4	1.77	0.20	55.7	2.32	0.29	42.7	2.17	0.10	63.0	2.28	0.26
2.90[c]	28.6	1.78	0.17	56.1	2.31	0.29	39.2	2.13	0.20	61.7	2.29	0.26
2.7	25.1	1.80	0.10	56.6	2.31	0.28	35.5	2.12	0.24	59.7	2.30	0.28
2.5	21.7	1.84	0.14	56.7	2.30	0.26	29.6	2.12	0.32	59.8	2.30	0.26
2.3	36.2	1.76	0.22	43.5	2.30	0.19	50.2	2.19	0.14	59.3	2.21	0.14
						WMC2						
3.0	31.7	1.76	0.10	66.7	2.21	0.23	34.4	2.30	0.14	54.7	2.36	0.32
2.856[b]	29.2	1.75	0.00	67.2	2.22	0.24	32.0	2.27	0.00	54.6	2.38	0.30
2.6	27.6	1.78	0.10	67.0	2.23	0.22	31.5	2.27	0.17	53.3	2.38	0.30
2.4	29.7	1.79	0.12	63.1	2.21	0.20	33.6	2.27	0.10	49.6	2.37	0.30
2.2	38.6	1.76	0.14	56.3	2.22	0.20	34.9	2.28	0.14	47.6	2.37	0.28
						FAD						
4.0	28.1	1.89	0.24	104.	4.12	1.05	45.3	2.58	0.26	75.9	2.77	0.50
3.84[b]	26.0	1.92	0.19	104.	4.07	1.02	42.0	2.56	0.20	76.8	2.80	0.52
3.6	23.0	1.97	0.16	103.	3.99	0.99	36.2	2.50	0.00	79.4	2.89	0.53
3.4	26.4	1.93	0.17	100.	4.07	1.01	44.1	2.58	0.28	71.6	2.79	0.48
3.2	33.1	1.85	0.27	98.6	4.21	1.07	51.8	2.61	0.37	66.1	2.71	0.44
						FFAC						
4.1	26.9	1.90	0.22	104.	4.12	1.05	43.5	2.58	0.28	79.1	2.84	0.52
3.95[c]	25.2	1.92	0.20	104.	4.09	1.03	40.7	2.57	0.22	79.8	2.86	0.54
3.8	23.8	1.95	0.14	104.	4.05	1.02	37.5	2.54	0.20	81.0	2.90	0.55
3.6	24.3	1.94	0.14	102.	4.06	1.01	41.8	2.57	0.26	76.1	2.89	0.53
3.4	27.3	1.91	0.20	101.	4.12	1.04	49.6	2.66	0.35	69.5	2.81	0.49

[a] Volume Vol (au), basin population N_i (e), and standard deviation of the population $\sigma(N_i)$. [b] Intermolecular distances defined in Table 1. [c] Equilibrium geometry.

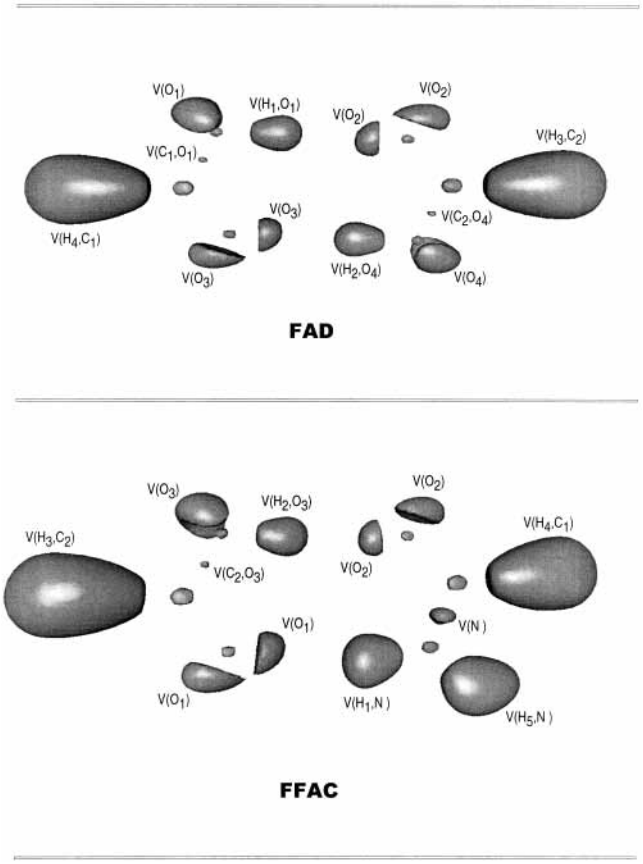

Figure 8. Localization domains ($\eta = 0.86$) of FAD and FFAC at equilibrium. Small unlabeled volumes at the location on oxygen, carbon, and nitrogen atoms belong to core basins. Relative orientation and atom numbering as in Figure 1.

Figure 8 (as a consequence of these selections for the illustrative purposes of Figures 7 and 8, some small intramolecular valence domains are unnoticed at the isosurfaces plotted). Note the position and orientation of disynaptic bond pair basins V(H,O) along the HB facing the monosynaptic lone pair basin V(O) of the acceptor oxygen. Lone pair basins show significant differences depending on whether oxygen is in the H-donor or in the H-acceptor monomer. The two lone pair basins in acceptor oxygens in Figure 7 (O_2 in WD and MWC1, O_1 in WMC2) are mutually more separated than those of donor oxygens. As noticed in Table 3, the two lone pair basins expected in donor oxygens in the cyclic dimers (O_1 and O_4 in FAD, O_3 in FFAC) are actually merged into one single monosynaptic basin with properties indicative of two lone pairs. These basins are seen in Figure 8 as a curved shape oriented at an approximately tetrahedral angle with respect to the H···O line. These effects suggest an internal shift in the space domain associated to the lone electron pair participating in the hydrogen bond, which agrees with local dipole effects observed before in HBs (see the discussion on this issue in ref 26).

We finally turn our attention to properties collected in Table 4 for valence basins involved in hydrogen bonding. This discussion intends to gauge the topological information provided by $\eta(\mathbf{r})$ when considering short intermolecular distances inside of equilibrium as a complement to the descriptors of $\rho(\mathbf{r})$ treated in the preceding section. Before analyzing this table, let us recall that the square of the standard deviation $\sigma(N_i)$, i.e., the variance, gives a measure of the uncertainty of the basin population whereas the magnitude $\sigma^2(N_i)/N_i$ (relative fluctuation of N_i) is interpreted as a measure of the electron delocalization within the basin.[36] "V(O-donor)" denotes either each one of the two lone pair basins of oxygen in the H-donor monomers in WD, MWC1, and WMC2 or the single total basin for the two lone

pairs in FAD and FFAC marked "V(O)[b]" in Table 3. "V_1(O-acceptor at HB)" represents the lone pair of oxygen in the H-acceptor pointing toward hydrogen (see Figures 7 and 8) whereas "V_2(O-acceptor)" is the basin of the second lone pair not directly involved in bonding. V(O,H) basins show populations N_i that increase very little at R below the equilibrium distance whereas their $\sigma(N_i)$ become much smaller, this trend inverting only at the shortest distances. If one compares Vol and $\sigma(N_i)$ values of this basin with the equivalent values of other V(O,H) basins not involved in the HB (Vol $\sim$ 55 au and $\sigma(N_i)$ $\sim$ 0.27 in both water and methanol; results not shown), data in Table 4 indicate that the electron localization domain for hydroxyl in donor monomers becomes strongly compacted upon hydrogen bonding (compare the relative sizes of $V(H_1,O_1)$ or $V(H_1,O_2)$ with other V(H,O) basins in Figure 7). If, additionally, one recalls that for these dimers the O−H bond elongates when the HB forms, these results indicate that the electron charge in this basin localizes at small domains shifted farther from the H atom. The behavior of this basin at the three first distances in Table 4 should then suggest that stronger hydrogen bonding could be expected at the third R, which shows the smallest values of Vol and $\sigma(N_i)$, yet this distance is inside of equilibrium. As noticed in the AIM analysis, these trends invert at the innermost distances where geometry distortions appear and the systems become dissociative.

Monosynaptic V(O-donor) properties remain nearly constant at distances near that at equilibrium, and only at the innermost separations do more significant changes arise: if one takes into account that these lone pairs do not participate directly in the HB interaction, this lack of sensibility is the expected result. However, marked differences between both lone electron pairs are noticed in the acceptor oxygens. The V_1(O) basin is much more compact than V_2(O) (see Vol data in Table 4 or compare sizes in Figures 7 and 8), and both its population and standard deviation are smaller than those of V_2(O). As a matter of fact, the values of Vol and $\sigma(N_i)$ for V_1(O) are actually the lowest ones among all the monosynaptic basins, which indicates quite compacted localization domains for this electron pair. The different features of both V(O-acceptor) basins can be rationalized as whether the domain V_1(O) participating in the HB were contracting and losing electron charge while pointing directly to the V(H,O) basin (see Figures 7 and 8), complying with the directional nature of hydrogen bonding. This contraction can be viewed as a consequence of the mutual penetration of H and acceptor O atoms occurring upon HB formation pointed out by Koch and Popelier[32] as part of their criteria to characterize HBs in the framework of AIM theory. Because these effects have been related with the strength of the HB interaction,[38] the change with R of V_1(O) properties should again suggest stronger hydrogen bonding at intermonomer distances shorter than that at equilibrium. The other lone pair V_2(O-acceptor) basin shows little variation at distances around that at equilibrium, which is expected if one considers that this localization domain is farther from the HB path.

The properties of valence basins of the ELF provide useful information to gain insight into the role played by electron pairs in hydrogen bonding complexes, which is especially valuable to translate the phenomenological picture of conventional "chemical intuition" into theoretically grounded quantitative descriptions. As suggested by the present discussion and previous reports,[36−38] clear relationships between relative HB strength and basin properties arise when *distinct* systems are compared. For instance, the sum of N_i values in Table 4 for V_1(O) and V_2(O) basins in the acceptor oxygen gives large populations that remain essentially constant at different distances but are closely related to the relative stabilities at equilibrium remarked before for these dimers. This highlights the essential role played by the lone pairs in increasing locally the electron charge of the electronegative acceptor atom upon formation of the HB. However, in agreement with that observed above for AIM indices obtained from the ED, except at very short distances where the systems destabilize strongly the topological descriptors of the ELF fail to provide a clear identification of the equilibrium structure among different intermolecular separations for a given HB system.

Summary and Conclusions

Ab initio MP2/6-311++G(d,p) calculations have been carried out on five dimers linked by one and two O−H···O hydrogen bonds to study the changes occurring in geometries and properties of $\rho(\mathbf{r})$ and $\eta(\mathbf{r})$ when the intermolecular distance R is shortened below the equilibrium value R_{eq}. Our goal was investigating how molecular properties instrumental to characterizing the nature of the HB vary with the intermonomer separation at short distances where strong hydrogen bonding should be expected. This goal was motivated by a great deal of reports in recent years, relating the strength of HBs (particularly O−H···O and O−H···N) to a variety of molecular properties dependent on $\rho(\mathbf{r})$ and $\eta(\mathbf{r})$.

At R about 0.2 Å shorter and longer than R_{eq}, geometries change very little and the energy remains within 1 kcal/mol above the minimum, but at 0.4 Å inside of R_{eq} the structures undergo dramatic changes. Dimers linked by one O−H···O bond turn from near linearity in the HB so as to display almost antiparallel OH groups, although remaining still below dissociation, and only at R as short as 2.2−2.3 Å (0.6 Å below R_{eq}) do they become strongly dissociative. The cyclic systems with two HBs distort significantly from the initial coplanarity at intermonomer separations about 0.4 Å shorter than R_{eq}. However, even at 0.6 Å closer, these destabilized dimers remain below dissociation due to the two HB interactions between their monomers.

Changes with R of AIM topological descriptors of $\rho(\mathbf{r})$ as well as values of the ED and electrostatic potential at the H nucleus continue to show the same trends inside of R_{eq} than outside and only at the closest intermonomer approximations where the systems suffer strong geometry distortions do these indices deviate from the previous trend and reveal loss of HB stability. Thus, values at the HB critical point of $\rho(\mathbf{r})$, ρ_C, and its Laplacian, $\nabla^2\rho_C$, continue to increase at $R < R_{eq}$, which calls for caution when one considers the correlations between these indices and HB strength frequently reported in the literature. Such correlations make sense only when used to study distinct HB systems, but they do not seem especially useful to distinguish between different intermolecular distances within a given system. A similar conclusion follows from the changes of local properties at the H nucleus, also often used as indices of HB strength. As for the total energy density at the BCP (H_C) whose sign provides information on the nature of an interaction insofar as covalent bonds always exhibit $H_C < 0$, increasingly negative values of H_C are found at distances inside of equilibrium and, again, only at close intermonomer proximities does H_C decrease its negative value or become positive.

Changes with R of properties of electron localization domains given by the basins of the ELF gradient field show a behavior rather similar to those of the ED. Populations and volumes of these basins allow us to identify the effects underlying HB interactions in terms of electron pairs. Thus, the bond pair

domain associated with the donor hydroxyl contracts and located at the H···O path shifted farther from H whereas lone pairs of the donor O exhibit virtually identical properties in dimers linked by one HB and merge at one single basin in dimers with two HBs. On the contrary, the two lone pairs of the acceptor O do show features rather different from the pair participating in the HB yielding a small domain pointing directly to hydrogen. The total electron charge obtained by adding the populations of both lone pair basins yields a large population in the acceptor O consistent with the traditional picture of HBs. However, the trend followed by the topological properties of $\eta(\mathbf{r})$ that could indicate stronger HBs continue at $R < R_{eq}$ and only for the distorted unstable geometries at closest approximations are significant changes suggesting a much weaker interaction noticed.

The usefulness of descriptors obtained from the topology of $\rho(\mathbf{r})$ and $\eta(\mathbf{r})$ in providing valuable information to understand the electron characteristics of hydrogen bonding has been largely demonstrated in the last years on HB dimers at equilibrium. However, their change with R within a given system shows that no special features which could help to distinguish equilibrium among other structures are identified at R_{eq} insofar as these properties continue to exhibit characteristic HB features inside of equilibrium. Except at very short R where strongly destabilized geometries arise, topological descriptors fail to identify the equilibrium structure. The results presented in this work suggest that the relationships involving these properties should be used with caution before being quantitatively applied to guess HB strength. Nonetheless, more work is necessary to establish whether particular topological indices can be unambiguously associated with the equilibrium structure. The ultimate physical nature of hydrogen bonding remains still a more elusive issue than suspected a few decades ago.

Acknowledgment. Dirección General de Investigación of the Spanish Ministerio de Ciencia y Tecnología is gratefully acknowledged for financial support under Project No. BQU2002-04005. Two anonymous referees are thanked for bringing to attention refs 44 and 57.

References and Notes

(1) Jeffrey, G. A. *An Introduction to Hydrogen Bonding*; Oxford University Press: Oxford, U.K., 1997.

(2) Scheiner, S. *Hydrogen Bonding: A Theoretical Perspective*; Oxford University Press: New York, 1997.

(3) Steiner, T. *Angew. Chem., Intl. Ed. Engl.* **2002**, *41*, 48.

(4) Grabowski, S. J. *J. Phys. Chem. A* **2001**, *105*, 10739.

(5) For a review see: (a) Alkorta, I.; Rozas, I.; Elguero, *J. Chem. Soc. Rev.* **1998**, *27*, 163. (b) Calhorda, M. J. *Chem. Commun.* **2000**, 801.

(6) Desiraju, G.; Steiner, T. *The Weak Hydrogen Bond in Structural Chemistry and Biology*; Oxford University Press: Oxford, U.K., 1999.

(7) Weiss, M. S.; Brandl, M.; Sühnel, J.; Pal, D.; Hilgenfeld, R. *Trends Biochem. Sci.* **2001**, *26*, 521.

(8) For a review see: Perrin, C. L.; Nielson, J. B. *Annu. Rev. Phys. Chem.* **1997**, *48*, 511.

(9) Gonzalez, L.; Mo, O.; Yañez, M.; Elguero, J. *J. Chem. Phys.* **1998**, *109*, 2685.

(10) Hao, X. Y.; Li, Z. R.; Wu, D.; Wang, Y.; Li, Z. S.; Sun, C. *J. Chem. Phys.* **2003**, *118*, 83.

(11) Kuo, J.; Ciobanu, C.; Ojamae, L.; Shavitt, I.; Singer, S. *J. Chem. Phys.* **2003**, *118*, 3583.

(12) Gilli, P.; Ferretti, V.; Bertolasi, V.; Gilli, G. *J. Am. Chem. Soc.* **1994**, *116*, 909.

(13) Humbel, S. *J. Phys. Chem. A* **2002**, *106*, 5517.

(14) Remer, L. C.; Jensen, J. H. *J. Phys. Chem. A* **2000**, *104*, 9266.

(15) Dannenberg, J. J.; Paraskevas, L. R.; Sharma, V. *J. Phys. Chem. A* **2000**, *104*, 6617.

(16) Arnold, W. D.; Oldfield, E. *J. Am. Chem. Soc.* **2000**, *122*, 12835.

(17) Mildvan, A. S.; Masiah, M. A.; Harris, T. K.; Marks, G. T.; Harrison, D. H. T.; Viragh, C.; Reddy, P. M.; Kovach, I. M. *J. Mol. Struct.* **2002**, *615*, 163.

(18) Vishveshwara, S.; Madhusudhan, M. S.; Maizel, J. V. *Biophys. Chem.* **2001**, *89*, 105.

(19) Cleland, W. W.; Kreevoy, M. M. *Science* **1994**, *264*, 1887.

(20) For a review on LBHBs in enzymes see: (a) Cleland, W. W.; Frey, P. A.; Gerlt, J. A. *J. Biol. Chem.* **1998**, *273*, 25529. (b) Cleland, W. W. *Archives Biochem. Biophys.* **2000**, *382*, 1.

(21) (a) Millen, D. J.; Legon, A. C.; Schrems, O. *J. Chem. Soc., Faraday Trans.2* **1979**, *75*, 592. (b) Legon, A. C.; Millen, D. J.; Rogers, S. C. *Proc. R. Soc. London Ser. A* **1980**, *370*, 213.

(22) (a) Kenyon, G. L.; Gerlt, J. A.; Petsko, G. A.; Kozarich, J.*Acc. Chem. Res.* **1995**, *28*, 178. (b) Gerlt, J. A.; Kreevoy, M. M.; Cleland, W. W., Frey, P. *Chem. Biol.* **1997**, *4*, 259. (c) Pan, Y.; McAllister, M. A. *J. Am. Chem. Soc.* **1998**, *120*, 166.

(23) (a) Warshel, A.; Papazyan, A.; Kollman, P. A. *Science* **1995**, *269*, 102. (b) Scheiner, S.; Kar, T. *J. Am. Chem. Soc.* **1995**, *117*, 6970.

(24) Ash, E. L.; Sudmeier, J. L.; De Fabo, E. C.; Bachovchin, W. W. *Science* **1997**, *278*, 1128.

(25) Galvez, O.; Gomez, P. C.; Pacios, L. F. *Chem. Phys. Lett.* **2001**, *337*, 263.

(26) Galvez, O.; Gomez, P. C.; Pacios, L. F. *J. Chem. Phys.* **2001**, *115*, 11166.

(27) Galvez, O.; Gomez, P. C.; Pacios, L. F. *J. Chem. Phys.* **2003**, *118*, 4878.

(28) Bader, R. F. W. *Atoms in Molecules. A Quantum Theory*; Clarendon Press: Oxford, U.K., 1990.

(29) Popelier, P. *Atoms in Molecules. An Introduction*; Prentice Hall: Harlow, 2000.

(30) Popelier, P. L. A.; Aicken, F. M.; O'Brien, S. E. In *Chemical Modelling: Applications and Theory*; The Royal Society of Chemistry: London, 2000; Vol. 1, Chapter 3.

(31) Popelier, P. L. A.; Smith, P. J. In *Chemical Modelling: Applications and Theory*; The Royal Society of Chemistry: London, 2002; Vol. 2, Chapter 8.

(32) Koch, U.; Popelier, P. L. A. *J. Phys. Chem.* **1995**, *99*, 9747.

(33) Becke, A. D.; Edgecombe, K. E. *J. Chem. Phys.* **1990**, *92*, 5397.

(34) Silvi, B.; Savin, A. *Nature* **1994**, *371*, 683.

(35) (a) Savin, A.; Silvi, B.; Colonna, F. *Can. J. Chem.* **1996**, *74*, 1088 (b) Savin, A.; Nesper, R.; Wengert, S. *Angew. Chem., Intl. Ed. Engl.* **1997**, *36*, 1809. (c) Beltran, A.; Andres, J.; Noury, S.; Silvi, B. *J. Phys. Chem. A* **1999**, *103*, 3078. (d) Fuster, F.; Savin, A.; Silvi, B. *J. Phys. Chem. A* **2000**, *104*, 852. (e) Fuentealba, P.; Savin, A. *J. Phys. Chem. A* **2001**, *105*, 11531. (f) Silvi, B.; Kryachko, E. S.; Tishchenko, O.; Fuster, F.; Nguyen, M. *Mol. Phys.* **2002**, *100*, 1659. (g) Chamorro, E.; Fuentealba, P.; Savin, A. *J. Comput. Chem.* **2003**, *24*, 496.

(36) Noury, S.; Colonna, F.; Savin, A.; Silvi, B. *J. Mol. Struct.* **1998**, *450*, 59.

(37) Fuster, F.; Silvi, B.; Berski, S.; Latajka, Z. *J. Mol. Struct.* **2000**, *555*, 75.

(38) Fuster, F.; Silvi, B. *Theor. Chem. Acc.* **2000**, *104*, 13.

(39) (a) Fuster, F.; Silvi, B. *Chem. Phys.* **2000**, *252*, 279. (b) Silvi, B. *J. Mol. Struct.* **2002**, *614*, 3.

(40) Jenkins, S.; Morrison, I. *Chem. Phys. Lett.* **2000**, *317*, 97.

(41) (a) Espinosa, E.; Molins, E.; Lecomte, C. *Chem. Phys. Lett.* **1998**, *285*, 170. (b) Espinosa, E.; Lecomte, C.; Molins, E. *Chem. Phys. Lett.* **1999**, *300*, 745. (c) Espinosa, E.; Molins, E. *J. Chem. Phys.* **2000**, *113*, 5686. (d) Espinosa, E.; Alkorta, I.; Rozas, I.; Elguero, J.; Molins, E. *Chem. Phys. Lett.* **2001**, *336*, 457.

(42) Alkorta, I.; Elguero, J. *J. Am. Chem. Soc.* **2002**, *124*, 1488.

(43) Rozas, I.; Alkorta, I.; Elguero, J. *J. Am. Chem. Soc.* **2000**, *122*, 11154.

(44) Grabowski, S. J.; Pogorzelska, M. *J. Mol. Struct.* **2001**, *559*, 201.

(45) Frisch, M. J.; Trucks, G. W.; Schlegel, H. B.; Scuseria, G. E.; Robb, M. A.; Cheeseman, J. R.; Zakrzewski, V. G.; Montgomery, J. A., Jr.; Stratmann, R. E.; Burant, J. C.; Dapprich, S.; Millam, J. M.; Daniels, A. D.; Kudin, K. N.; Strain, M. C.; Farkas, O.; Tomasi, J.; Barone, V.; Cossi, M.; Cammi, R.; Mennucci, B.; Pomelli, C.; Adamo, C.; Clifford, S.; Ochterski, J.; Petersson, G. A.; Ayala, P. Y.; Cui, Q.; Morokuma, K.; Malick, D. K.; Rabuck, A. D.; Raghavachari, K.; Foresman, J. B.; Cioslowski, J.; Ortiz, J. V.; Baboul, A. G.; Stefanov, B. B.; Liu, G.; Liashenko, A.; Piskorz, P.; Komaromi, I.; Gomperts, R.; Martin, R. L.; Fox, D. J.; Keith, T.; Al-Laham, M. A.; Peng, C. Y.; Nanayakkara, A.; Gonzalez, C.; Challacombe, M.; Gill, P. M. W.; Johnson, B.; Chen, W.; Wong, M. W.; Andres, J. L.; Head-Gordon, M.; Replogle, E. S.; Pople, J. A. *GAUSSIAN98*; Gaussian Inc.: Pittsburgh, PA, 1998.

(46) Biegler-Konig, F. W.; Bader, R. F. W.; Tang, T. H. *J. Comput. Chem.* **1982**, *3*, 317.

(47) Pacios, L. F. *Comput. Biol. Chem.* **2003**, *27*, 197.

(48) Noury, S.; Krokidis, X.; Fuster, F.; Silvi, B. *Comput. Chem.* **1999**, *23*, 597.

(49) Weber, S. *JMap3D.* http://jcrystal.com/steffenweber/JAVA/JMAP3D/JMAP3D.html.

(50) (a) Grabowski, S. J. *J. Phys. Chem. A* **2000**, *104*, 5551. (b) Grabowski, S. J. *Chem. Phys. Lett.* **2001**, *338*, 361.

(51) Espinosa, E.; Alkorta, I.; Elguero, J.; Molins, E. *J. Chem. Phys.* **2002**, *117*, 5529.
(52) Flaig, R.; Koritsanszky, T.; Dittrich, B.; Wagner, A.; Luger, P. *J. Am. Chem. Soc.* **2002**, *124*, 3407.
(53) Popelier, P. L. A. *Coord. Chem. Rev.* **2000**, *197*, 169.
(54) Gillespie, R. J.; Popelier, P. L. A. *Chemical Bonding and Molecular Geometry. From Lewis to Electron Densities*; Oxford University Press: New York, 2001.
(55) (a) Hobza, P.; Havlas, Z. *Chem. Rev.* **2000**, *100*, 4253. (b) Hermansson, K. *J. Phys. Chem. A* **2002**, *106*, 4695.
(56) Li, X.; Liu, L.; Schlegel, H. B. *J. Am. Chem. Soc.* **2002**, *124*, 9639.
(57) Alabugin, I. V.; Manoharan, M.; Peabody, S.; Weinhold, F. *J. Am. Chem Soc.* **2003**, *125*, 5973.
(58) Politzer, P.; Murray, J. S. *Theor. Chem. Acc.* **2002**, *108*, 134.
(59) Politzer, P.; Parr, R. G. *J. Chem. Phys.* **1974**, *61*, 4258.
(60) (a) Dimitrova, V.; Ilieva, S.; Galabov, B. *J. Phys. Chem. A* **2002**, *106*, 11801. (b) Galabov, B.; Bobadova-Parvanova, P.; Ilieva, S.; Dimitrova, V. *J. Mol. Struct. (THEOCHEM)* **2003**, *630*, 101.
(61) Parr, R. G.; Yang, W. *Density Functional Theory of Atoms and Molecules*; Oxford University Press: New York, 1989.
(62) Savin, A.; Jepsen, O.; Flad, J.; Andersen, O. K.; Preuss, H.; von Schnering, H. G. *Angew. Chem., Intl. Ed. Engl.* **1992**, *31*, 187.